



Universiteit
Leiden
The Netherlands

The stress connection: Neuroimaging studies of emotion circuits in social stress, personality, and stress-related psychopathology

Veer, I.M.

Citation

Veer, I. M. (2015, January 27). *The stress connection: Neuroimaging studies of emotion circuits in social stress, personality, and stress-related psychopathology*. Retrieved from <https://hdl.handle.net/1887/31594>

Version: Corrected Publisher's Version

License: [Licence agreement concerning inclusion of doctoral thesis in the Institutional Repository of the University of Leiden](#)

Downloaded from: <https://hdl.handle.net/1887/31594>

Note: To cite this publication please use the final published version (if applicable).

Cover Page



Universiteit Leiden



The handle <http://hdl.handle.net/1887/31594> holds various files of this Leiden University dissertation

Author: Veer, Ilja Milos

Title: The stress connection : neuroimaging studies of emotion circuits in social stress, personality, and stress-related psychopathology

Issue Date: 2015-01-27

CHAPTER 5

Whole brain resting-state analysis reveals decreased functional connectivity in major depression

Veer, I. M., Beckmann, C. F., van Tol, M. J., Ferrarini, L., Milles, J., Veltman, D. J., Aleman, A., van Buchem, M. A., van der Wee, N. J., & Rombouts, S. A. R. B. (2010). *Frontiers in Systems Neuroscience*, 4, 41.

ABSTRACT

Recently, both increases and decreases in resting-state functional connectivity have been found in major depression. However, these studies only assessed functional connectivity within a specific network or between a few regions of interest, while comorbidity and use of medication was not always controlled for. Therefore, the aim of the current study was to investigate whole-brain functional connectivity, unbiased by *a priori* definition of regions or networks of interest, in medication-free depressive patients without comorbidity. We analyzed resting-state fMRI data of 19 medication-free patients with a recent diagnosis of major depression (within 6 months before inclusion) and no comorbidity, and 19 age- and gender-matched controls. Independent component analysis was employed on the concatenated data sets of all participants. Thirteen functionally relevant networks were identified, describing the entire study sample. Next, individual representations of the networks were created using a dual regression method. Statistical inference was subsequently done on these spatial maps using voxel-wise permutation tests. Abnormal functional connectivity was found within three resting-state networks in depression: 1) decreased bilateral amygdala and left anterior insula connectivity in an affective network, 2) reduced connectivity of the left frontal pole in a network associated with attention and working memory, and 3) decreased bilateral lingual gyrus connectivity within ventromedial visual regions. None of these effects were associated with symptom severity or gray matter density. We found abnormal resting-state functional connectivity not previously associated with major depression, which might relate to abnormal affect regulation and mild cognitive deficits, both associated with the symptomatology of the disorder.

INTRODUCTION

Patients suffering from a major depressive episode typically show pervasive depressed mood or anhedonia, accompanied by several cognitive and physical symptoms (APA, 1994). The apparent heterogeneity in depressive symptom domains (i.e., mood, cognition, motor, and vegetative) is unlikely to be explained by the (functional) breakdown of a single brain area (Davidson, Pizzagalli, Nitschke, & Putnam, 2002). It has thus been proposed that depressive symptoms are associated with dysregulation of a brain network encompassing large parts of the prefrontal cortex (PFC), limbic areas, and subcortical structures (Mayberg, 1997; 2003).

Based on data from blood flow and glucose metabolism SPECT and PET studies, and more recently task-related functional MRI (fMRI) studies, current models for depression postulate that ventral and dorsal subsystems of this brain network are differentially affected in this disease (Drevets et al., 2008; Mayberg, 2003). An imbalanced functional integration of these subsystems may lead to a heightened response to negative information in ventral regions (bottom–up) on the one hand, and a failure to regulate this response through dorsal regions (top–down) on the other hand (Phillips, Drevets, Rauch, & Lane, 2003b). For example, engagement of lateral PFC regions has been linked to efficient top–down regulation of affective responses (Dolcos & McCarthy, 2006; Pessoa, 2008), a mechanism that has been shown to fail in patients suffering depression (Johnstone et al., 2007).

Over the last decade, studying such functional interactions between brain regions or systems has become increasingly important for understanding the dynamic interactions between neural systems in both health and disease (Stephan, Riera, Deco, & Horwitz, 2008). In depression, several studies have shown abnormal functional connectivity (FC) during both cognitive and emotional task paradigms (Chen et al., 2008; Johnstone et al., 2007; Matthews, Strigo, Simmons, Yang, & Paulus, 2008; Urry et al., 2006), which have already provided valuable insights on how dysfunctional interactions between brain regions may relate to abnormal behavioral response patterns in depressed patients. However, it might also be beneficial to explore whether these connections are compromised in the absence of goal-directed (i.e., task-induced)

behavior. For example, resting-state (RS; i.e., without external task demands) FC may be able to predict how the brain responds to an externally cued task (Mennes et al., 2010). Studies employing RSFC have shown to be successful in mapping large-scale connectivity patterns in the brain (Biswal et al., 1995; Fox & Raichle, 2007; Lowe, Mock, & Sorenson, 1998). In addition, these so-called resting-state networks (RSNs) are found consistently across participants and over time (Damoiseaux et al., 2006; Shehzad et al., 2009) and show a remarkable overlap with patterns of task-induced activity (Smith et al., 2009).

RS-fMRI studies in major depression have recently reported on altered FC in several areas within the proposed network model of depression (Drevets et al., 2008; Mayberg, 1997). Decreased connectivity of the dorsal anterior cingulate cortex (ACC) with the medial thalamus and left pallidostriatum was found in patients suffering from depression, and a trend for decreased connectivity between the ACC and the amygdala (Anand, Li, Wang, Wu, Gao, Bukhari, Mathews, Kalnin, & Lowe, 2005b; 2005a). In another study, depressive patients were found to show increased connectivity of the subgenual ACC (cg25) and the thalamus within the default mode network (DMN) (Greicius et al., 2007), a canonical RSN (Greicius et al., 2003; Raichle et al., 2001). This finding was partially confirmed by a recent study showing unique cg25, but not thalamic, connectivity within the DMN in the depression group (Zhou et al., 2010). It must be noted, however, that for this effect only qualitative comparisons were carried out between the groups. Additionally, these researchers found increased intra-network connectivity in depression between regions of the DMN, and within the task positive network (TPN), associated with attention and working memory (Fox et al., 2005), together with increased anticorrelations between regions of the two networks (Zhou et al., 2010). A last study did not show any FC differences between major depressive disorder (MDD) patients and controls using conventional statistics (Craddock, Holtzheimer, Hu, & Mayberg, 2009). However, the authors were able to discriminate between patients and controls using support vector classification. In addition to the altered FC found in several task-related fMRI studies, these RS findings further support the idea of dysfunctional interactions as a core feature of depressive symptomatology.

To date, RS-fMRI studies focusing on depression examined connectivity in a limited number of predefined regions or networks of interest, thereby not fully exploring the data as acquired with RS-fMRI. That is, recent studies have identified several other networks of simultaneously oscillating brain regions (Beckmann, DeLuca, Devlin, & Smith, 2005; Damoiseaux et al., 2006), which may represent multiple functional domains. Furthermore, in some of the studies in MDD, comorbidity and use of medication could not be ruled out as potential confounders.

The aim of the present study was to investigate FC patterns using RS-fMRI in medication-free patients with MDD without comorbidity, and carefully matched healthy controls. Rather than focusing on predefined regions or networks of interest, we adopted an inclusive (exploratory) approach by investigating whole-brain RS-fMRI FC at the network level, ensuring the optimal use of the wealth of information present in the data. Based on the current neurobiological models for depression and the RS studies described above, we expected that altered connectivity would be observed in those RSNs that include areas known to be associated with affective (including ventral prefrontal cortex and limbic areas) and more cognitive (including lateral prefrontal and parietal areas) processing, as well as RSNs that show cortico-striatal connectivity.

METHODS

Participants

Participants were selected from the MRI study of the large-scale longitudinal multi-center Netherlands Study on Depression and Anxiety (NESDA; www.nesda.nl) (Penninx et al., 2008), which is designed to examine the long-term course and consequences of depression and anxiety disorders. Participants were recruited through general practitioners, primary care and specialized mental care institutions. For the current study, all participants were required to be fluent in Dutch and right-handed. Patients were included when they met the following criteria: 1) a recent diagnosis (i.e., within 6 months before inclusion) of MDD as indexed by the fourth edition of

Table 5.1 Demographic and clinical characteristics for the study sample.

	healthy controls (<i>n</i> = 19)	major depressive disorder (<i>n</i> = 19)
Age	36.11 ± 10.56 (21-53) y/o	36.21 ± 9.7 (20-57) y/o
Gender	8 male/11 female	8 male/11 female
Education *	14 ± 2.67 (9-18) years	12.21 ± 2.35 (9-18) years
MADRS **	0.63 ± 1.07 (0-3)	14.21 ± 9.62 (0-33)

Note: MADRS = Montgomery-Asberg depression rating scale. Except for sex, all values are mean ± *SD* (range). * $p < .05$, ** $p < .001$, using independent sample *t*-tests.

the diagnostic and statistical manual of mental disorders (DSM-IV) (APA, 1994), based on the Composite Interview Diagnostic Instrument (CIDI; lifetime version 2.1), administered by a trained clinical interviewer, 2) no current comorbidity with other DSM-IV axis-1 disorders, and 3) no use of psychotropic medication. Exclusion criterion for controls was a history of any DSM-IV axis-1 disorder based on the CIDI. Axis-2 disorders were not assessed in this study. Exclusion criteria for all participants were: 1) daily use of medication or other substances known to affect the central nervous system; 2) the presence or history of major internal or neurological disorders; 3) history of dependency on or recent abuse of alcohol and/or drugs (i.e., in the past year) as diagnosed with the CIDI; 4) hypertension; 5) general MRI-contraindications. None of the included patients underwent treatment for depression.

For the present study, imaging data were available from 23 MDD patients who fulfilled the aforementioned criteria. Two patients were removed from the sample due to excessive head motion during scan acquisition (> 3 mm in any of the acquired volumes). Two other patients were removed because no proper age-matched healthy control (HC) was available. For each of the remaining 19 MDD patients, we included in a pair-wise fashion an age- and sex-matched healthy control subject, although education was higher in controls (see **Table 5.1**). The mean Montgomery-Asberg depression rating scale (MADRS) (Montgomery & Asberg, 1979) symptom severity score for the MDD group was 14.21, *SD* 9.62, with five participants considered to be in remission (MADRS score < 10) at the time of the imaging study. Written informed

consent was obtained from all participants and none received compensation except for reimbursement of travel expenses. The study was approved by the Central Ethics Committees of the three participating medical centers (i.e., Leiden University Medical Center [LUMC], Amsterdam Medical Center [AMC], and University Medical Center Groningen [UMCG]).

MATERIALS

Data acquisition

Participants were scanned at one of the three participating centers within 8 weeks after completion of NESDA baseline interview (Penninx et al., 2008). RS-fMRI data were acquired at the end of the fixed imaging protocol: after completion of three task-related functional MRI runs (to be reported elsewhere), and the acquisition of an anatomical scan (scan sequence: Tower of London, word encoding, T_1 -weighted scan, word recognition, perception of facial expression). In the darkened MR room participants were instructed to lie still with their eyes closed and not to fall asleep. Compliance to these instructions was verified as part of the exit interview.

Imaging data were acquired on a Philips 3T Achieva MRI scanner using a six- (Amsterdam) or eight-channel (Groningen and Leiden) SENSE head coil for radiofrequency reception (Philips Healthcare, Best, The Netherlands). RS-fMRI data were acquired using T_2^* -weighted gradient-echo echo-planar imaging with the following scan parameters in Amsterdam and Leiden: 200 whole-brain volumes; repetition time (TR) = 2300 ms; echo time (TE) = 30 ms; flip angle = 80° ; 35 axial slices; no slice gap; FOV = 220×220 mm; in plane voxel resolution = $2.3 \text{ mm} \times 2.3 \text{ mm}$; slice thickness = 3 mm; same in Groningen, except: TE = 28 ms; 39 axial slices; in plane voxel resolution = $3.45 \text{ mm} \times 3.45 \text{ mm}$. For registration purposes and analysis of gray matter density, a high-resolution T_1 -weighted image was acquired with the following scan parameters: repetition time (TR) = 9 ms; echo time (TE) = 3.5 ms; flip angle = 80° ; 170 sagittal slices; no slice gap; FOV = 256×256 mm; in plane voxel resolution = $1 \text{ mm} \times 1 \text{ mm}$; slice thickness = 1 mm.

Data preprocessing

The preprocessing of RS-fMRI images was carried out using FEAT (FMRI Expert Analysis Tool) Version 5.90, part of FSL (FMRIB's Software Library; www.fmrib.ox.ac.uk/fsl) (Smith et al., 2004). The following processing steps were applied: motion correction (Jenkinson et al., 2002), removal of non-brain tissue (Smith, 2002), spatial smoothing using a Gaussian kernel of 4-mm full width at half maximum, grand-mean intensity normalization of the entire 4D dataset by a single multiplicative factor, high-pass temporal filtering (Gaussian-weighted least-squares straight line fitting, with $\sigma = 50$ s (i.e., 0.01 Hz cut-off), and registration to the high resolution T_1 and MNI-152 standard space (T_1 standard brain averaged over 152 subjects; Montreal Neurological Institute, Montreal, QC, Canada) images (Jenkinson et al., 2002; Jenkinson & Smith, 2001). Normalized 4D data sets were subsequently resampled to 4 mm isotropic voxels to reduce computational burden in the following analysis steps.

Extracting resting-state networks

Standard group independent component analysis (ICA) was carried out using probabilistic ICA (PICA) (Beckmann & Smith, 2004), as implemented in FSL's MELODIC tool, Version 3.09. Default group PICA processing steps were applied to the individual preprocessed and normalized data sets: masking out non-brain voxels, voxel-wise de-meaning of the data, and normalization of the voxel-wise variance based on all data sets. Subsequently, data sets from both MDD patients and HCs were concatenated in time to create a single 4D data set, which was then projected into a 20-dimensional subspace using principal component analysis. Next, the data set was decomposed into 20 sets of independent vectors, which describe signal variation across the temporal (time-courses) and spatial (maps) domain by optimizing for non-Gaussian spatial source distributions using the FastICA algorithm (Hyvärinen, 1999). At this model order selection, it has been shown that most of the frequently observed large-scale RSNs can be discerned in the data when using this method (Abou Elseoud et al., 2010). The resulting estimated component maps were divided by the standard deviation of the residual noise and thresholded at a posterior probability threshold of $p > .5$ (i.e., an equal loss is placed on false positives and false negatives)

by fitting a Gaussian/Gamma mixture model to the histogram of intensity values (Beckmann & Smith, 2004).

Statistical analyses

Subject specific statistical maps were created to test for differences between the MDD and HC groups in the identified components. This was done adopting a dual regression procedure (as previously described in: Filippini et al., 2009). In short, multiple linear regression of the z -thresholded Group PICA maps against the preprocessed individual 4D resampled data sets yielded a subject specific time course for each of the group components. Next, multiple linear regression of these time courses was carried out against the preprocessed individual 4D data sets in the standard space resolution (i.e., 2 mm), thereby providing better spatial specificity. This resulted in subject specific z -maps for each of the 20 group components.

Prior to statistical inference 13 out of the 20 components were identified as anatomically and functionally relevant RSNs upon visual inspection, the seven others reflecting distinct artifacts resulting from head motion, fluctuations in cerebrospinal fluid, and physiological or scanner noise. Criteria for inclusion were: signal within the low frequency range of 0.1–0.01 Hz (Cordes et al., 2001; Lowe et al., 1998), connectivity patterns were mainly located in gray matter, and presence of coherent clusters of voxels (De Martino et al., 2007). Inference was carried out only on the subject specific z -maps of the 13 relevant RSNs. Statistical difference was assessed non-parametrically using FSL's Randomize tool, Version 2.1, incorporating threshold-free cluster enhancement (TFCE) (Smith & Nichols, 2009). Besides modeling regressors for each of the two groups, additional nuisance regressors describing scanner location and age were added to the model. Separate null distributions of t -values were derived for the contrasts reflecting the between and within group effects by performing 5000 random permutations and testing the difference between groups or against zero for each iteration (Nichols & Holmes, 2002). For each RSN, the resulting statistical maps were thresholded at $p < .05$ (TFCE-corrected for family-wise errors) for the group main effects. Between-group effects were thresholded controlling the local false discovery rate (FDR) (Efron, 2004; Filippini et al., 2009) at $q < .01$, and subsequently spatially

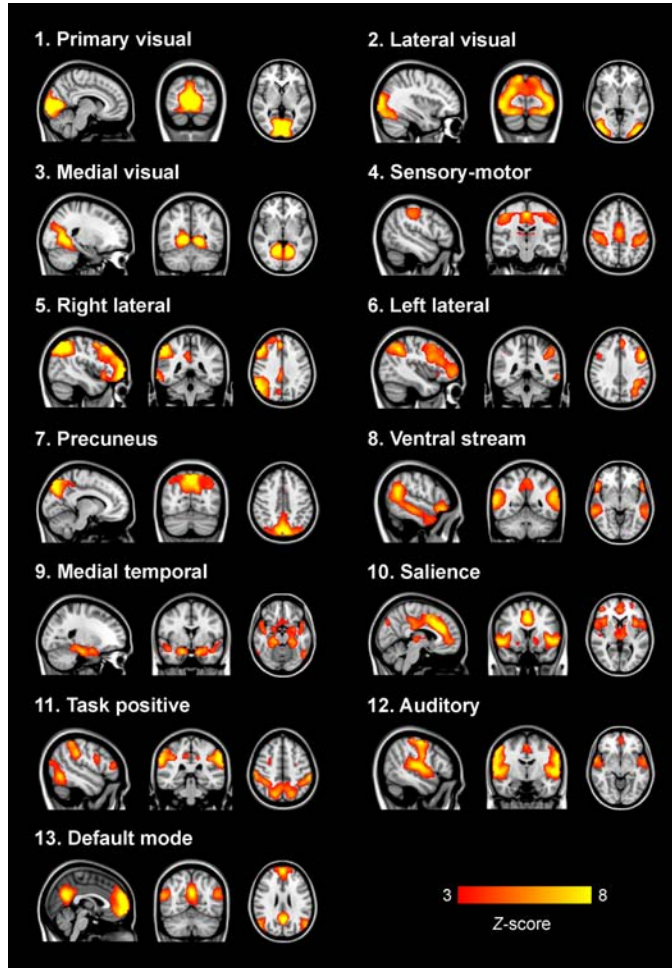


Figure 5.1 Depicted here are the 13 functionally relevant RSNs resulting from the group PICA step carried out on the concatenated data sets from both patients and controls. Most networks have previously been described (for example in: Beckmann et al., 2005; Damoiseaux et al., 2006) and show assemblies of regions associated with sensory processing, affective processing, and higher order cognitive processes. Images are z-statistics, ranging from 3 to 8, overlaid on the 2 mm MNI-152 standard brain. The left hemisphere of the brain corresponds to the right side in this image.

masked with a binary representation of the conjunction of the group main effects images. Note that we applied a more stringent FDR threshold than the more generally accepted $q \leq .05$, together with masking for the group main effects, to decrease susceptibility to Type I errors when testing multiple RSNs.

Gray matter morphology

Major depressive disorder-related gray matter (GM) abnormalities have been found previously in several regions of the brain, although not always consistently (Lorenzetti, Fornito, Allen, & Yücel, 2009; Sheline, 2003). To test whether altered FC in the present study might be explained by MRI-detectable loss of gray matter, a VBM style analysis was run on the acquired high-resolution T_1 -weighted data sets (Ashburner & Friston, 2000; Good et al., 2001). Using FSL's VBM toolbox, all structural images were first brain extracted, then tissue-type segmented, normalized to MNI-152 standard space and non-linearly registered to each other (e.g., Douaud et al., 2007). Next, standard space binary masks were created from the voxels that covered each RSN (conjunction of the FWE-corrected $HC > 0$ and $MDD > 0$ contrast maps) as well as from voxels showing differences between the two groups within the separate networks (local FDR controlled $HC > MDD$ and $MDD > HC$ contrast maps). The binary masks were then used to extract mean gray matter intensity scores within these masks for each of the participants. To rule out the influence of any subtle GM density variations, we included the GM values, from both the difference masks and the RSN as a whole, as regressors in the statistical model (see, e.g., Damoiseaux et al., 2008). Additionally, using SPSS Version 16.0 (SPSS Inc.) between-group t -tests were carried out on the participants' mean intensity scores derived from each mask to test whether the two groups differed in GM density on average. Note that whole brain VBM results of a large sample (including MDD) from the NESDA study is reported elsewhere (van Tol et al., 2010).

RESULTS

Resting-state functional connectivity

Thirteen functionally relevant RSNs were found using the group PICA analysis (**Figure 5.1**). Most of these networks have been described in previous studies using similar methodology and were shown to be stable across participants and over time (Beckmann et al., 2005; Damoiseaux et al., 2006). The assemblies of brain areas shown in these networks covered the primary [1], lateral [2] and medial visual cortex [3], sensory-motor cortex [4], ventral stream [8] auditory cortex [12], the hippocampus-amygdala complex [9], precuneus [7] together with the DMN [13], a network associated with salience processing (Seeley, Menon, et al., 2007b) [10], and networks encompassing areas associated with higher order cognition such as attention [11] and working memory [5, 6].

The presence of all 13 networks found with PICA was confirmed in both the HC and MDD group by testing the main effects of group on the subject specific z -maps of these networks (all $p < .05$, TFCE and FWE-corrected). Between-group differences in the voxel-wise spatial distribution of the FC maps were subsequently revealed in three networks (local FDR-corrected at $q \leq .01$) (see **Figure 5.2** and **Tables 5.2-5.4**).

Within these networks nearly all differences indicated decreased FC in the MDD group. The first network showed an assembly of functionally connected regions in the auditory cortex (Heschl's gyrus) bilaterally, extending into the pre- and post-central gyri, as well as more ventral areas known to be involved in affective processing, including the insula and temporal poles bilaterally, the medial PFC (BA 10), and bilateral amygdala. Whereas the amygdala and left insula showed connectivity with the rest of the network in HCs, these regions showed decreased FC in the depressed group.

In addition, increased FC in the MDD group was found in the right inferior frontal gyrus (IFG) within this RSN (**Figure 5.2a and 5.2b**, RSN 12). The second network mainly showed FC within the lateral parietal cortex, temporal-occipital junction, and precentral gyrus, which are areas involved in attention and working

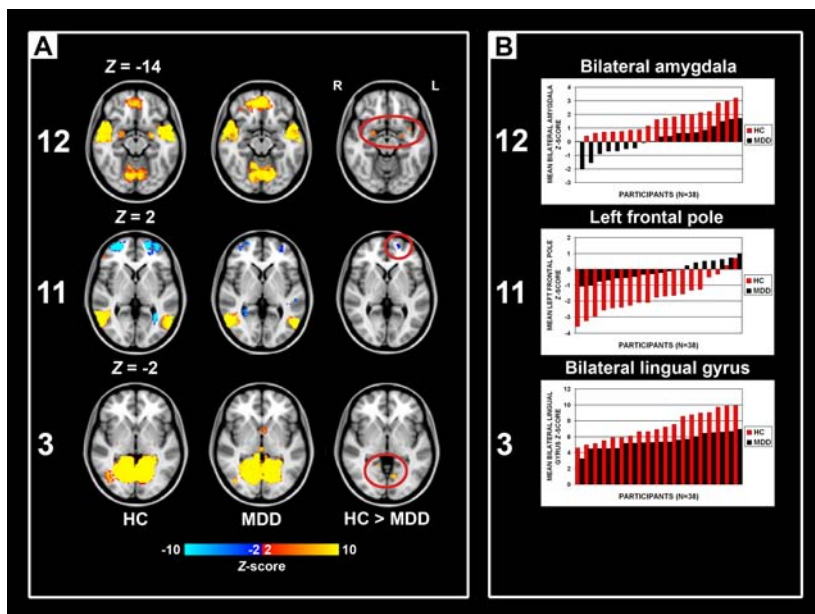


Figure 5.2 Group main effects and between-group effects. Numbering corresponds to the networks depicted in **Figure 5.1**. **(A)** Depicted here are the group main and between-group effects for three RSNs. Group main effects are corrected for family-wise errors ($p < .05$) and between-group effects are corrected according to a local false discovery rate of 1 %. RSN 12 shows an assembly of ventral affective regions, such as temporal poles, insula, medial prefrontal cortex, and amygdala, the latter two regions demonstrating decreased connectivity within the MDD group. RSN 11 shows brain regions linked to attention, of which the left frontal pole shows decreased connectivity in the MDD group. RSN 3 shows MDD-related decreased connectivity of the bilateral lingual gyrus with other medial visual areas. Images are z-statistics, ranging from 2 to 10, overlaid on the 2 mm MNI-152 standard brain. The left hemisphere of the brain corresponds to the right side in this image. HC, healthy controls; MDD, major depressive disorder. **(B)** Distribution of the mean individual z-scores within the bilateral amygdala (12), left frontal pole (11), and bilateral lingual gyrus (3). Depicted in red are the controls, in black the MDD group, both sorted from smallest to highest z-value.

memory. In addition, the frontal poles were found to be negatively associated with the time course of this network. Reduced FC of the left frontal pole was demonstrated in

Table 5.2 RSN 12 characteristics and statistics.

Region	coordinates (MNI space)			p_{FWE}		$p_{local\ FDR}$	
	x	y	z	HC	MDD	HC > MDD	MDD > HC
Positive							
left cerebellum	-16	-68	-22	.002	<.001	ns	ns
right cerebellum	18	-68	-22	<.001	<.001	ns	ns
left superior temporal gyrus	-44	0	-14	<.001	<.001	ns	ns
right superior temporal gyrus	-46	-30	6	<.001	<.001	ns	ns
left amygdala	52	4	-14	<.001	<.001	<.001	ns
right amygdala	58	-32	6	<.001	<.001	ns	ns
left/right medial prefrontal cortex	-24	-6	-14	.007	<.001	<.001	ns
left insula	24	-4	-16	.02	ns	<.001	ns
right insula	0	48	-14	.005	<.001	ns	ns
right thalamus	-40	-6	-2	<.001	<.001	ns	ns
left/right anterior cingulate gyrus	-36	4	-18	<.001	ns	<.001	ns
left pre- and postcentral gyrus	38	-6	6	<.001	<.001	ns	ns
right pre- and postcentral gyrus	12	-22	0	ns	.008	ns	ns
left/right postcentral gyrus	0	2	38	<.001	<.001	ns	ns
right inferior frontal gyrus	-44	-20	44	<.001	<.001	ns	ns
left thalamus	48	-16	44	<.001	<.001	ns	ns
left middle frontal gyrus	0	-26	50	.002	<.001	ns	ns
left precentral gyrus	56	24	16	ns	<.001	ns	<.001
Negative							
left thalamus	-12	-6	12	ns	.039	ns	ns
left middle frontal gyrus	-28	32	36	.01	ns	ns	ns
left precentral gyrus	-28	6	48	ns	.026	ns	ns

Note: group main effects are FWE-corrected for multiple comparisons, between group contrasts are corrected for multiple comparisons using a local false discovery rate (FDR) of 1 %. HC = healthy controls, MDD = major depressive disorder, ns = not significant.

the MDD group (**Figure 5.2a and 5.2b**, RSN 11). The third network showed functionally integrated areas within the medial occipital cortex, mostly covering Brodmann area 19, involved in visual processing. Although both controls and depressed participants demonstrated this connectivity pattern, a consistent decrease in functional integration of the lingual gyrus was found bilaterally in the MDD group in this RSN (**Figure 5.2a and 5.2b**, RSN 3).

The wide range in MADRS scores in the patient group allowed us to examine the relation between current symptom severity and the strength of the function-

Resting-state functional connectivity in major depression

Table 5.3 RSN 11 characteristics and statistics.

Region	coordinates (MNI space)			p_{FWE}		$p_{local\ FDR}$	$p_{local\ FDR}$
	x	y	z	HC	MDD	HC > MDD	MDD > HC
Positive							
left inferior temporal gyrus	-48	-62	-12	<.001	<.001	ns	ns
right inferior temporal gyrus	54	-60	-8	<.001	<.001	ns	ns
left lateral occipital cortex	-40	-80	18	<.001	<.001	ns	ns
right lateral occipital cortex	44	-72	14	<.001	<.001	ns	ns
left supramarginal gyrus	-56	-28	24	<.001	<.001	ns	ns
	-46	-38	40	<.001	<.001	ns	ns
right supramarginal gyrus	58	-40	24	<.001	<.001	ns	ns
	40	-38	40	<.001	<.001	ns	ns
left posterior cingulate cortex	-10	-38	40	<.001	<.001	ns	ns
right posterior cingulate cortex	12	-38	42	<.001	<.001	ns	ns
left middle frontal gyrus	-46	36	12	.025	ns	ns	ns
right middle frontal gyrus	50	40	8	.028	ns	ns	ns
right precentral gyrus	48	8	26	.035	ns	ns	ns
left/right anterior cingulate gyrus	2	2	32	.037	ns	ns	ns
Negative							
left hippocampus	-28	-24	-16	.002	ns	ns	ns
left middle temporal gyrus	-58	-30	-10	.002	.002	ns	ns
right middle temporal gyrus	58	-20	-10	.003	ns	ns	ns
left frontal pole	-24	56	-4	<.001	ns	ns	<.001
right frontal pole	32	56	-2	<.001	<.001	ns	ns
left paracingulate gyrus	-8	32	36	.003	ns	ns	ns
right paracingulate gyrus	4	32	38	.003	.003	ns	ns
left middle frontal gyrus	-36	16	38	ns	<.001	ns	ns
left/right cuneus	2	-78	36	<.001	<.001	ns	ns

Note: group main effects are FWE-corrected for multiple comparisons, between group contrasts are corrected for multiple comparisons using a local false discovery rate (FDR) of 1 %. HC = healthy controls, MDD = major depressive disorder, ns = not significant.

al connections with the areas showing abnormal connectivity in this study. Within the depression group, Pearson correlation coefficients were calculated between the MADRS scores and the individual z-scores obtained from the affected areas within the corresponding individual component maps. However, no association was found between FC strength and symptom severity in any of these regions.

Table 5.4 RSN 3 characteristics and statistics.

Region	coordinates (MNI space)			p_{FWE}	$p_{local\ FDR}$	$p_{local\ FDR}$	
	x	y	z	HC	MDD	HC > MDD	MDD > HC
Positive							
left lingual gyrus	-10	-68	-2	<.001	<.001	<.001	ns
right lingual gyrus	16	-68	-2	<.001	<.001	ns	ns
	16	-50	-2	<.001	<.001	<.001	ns
left lateral occipital cortex	-38	-76	22	<.001	<.001	ns	ns
right lateral occipital cortex	50	-72	16	.013	<.001	ns	ns
left cuneus	-14	-76	22	<.001	<.001	ns	ns
right cuneus	18	-76	22	<.001	<.001	ns	ns
right precentral gyrus	40	8	28	ns	.03	ns	ns
left caudate nucleus	-6	8	4	ns	.011	ns	ns
right caudate nucleus	8	8	4	ns	.016	ns	ns

Note: group main effects are FWE-corrected for multiple comparisons, between group contrasts are corrected for multiple comparisons using a local false discovery rate (FDR) of 1 %. HC = healthy controls, MDD = major depressive disorder, ns = not significant.

Gray matter results

No differences in mean gray matter were observed between controls and depressed participants in any of the three RSNs as a whole, or in the areas showing between-group differences within these RSNs, all $t(36) < 1$, $p > .3$. In addition, adding GM density values as covariates in the statistical model did not change the functional connectivity results as described in the previous section. This indicates that the altered FC within the three networks is unlikely to be related to macroscopic (i.e., MRI observable) gray matter abnormalities.

DISCUSSION

In the present study we set out to investigate differences in whole brain FC between medication-free MDD patients without comorbidity, and a group of age- and sex-matched healthy controls using RS-fMRI. It was expected that altered connectivity would be observed in those RSNs which contain regions previously described to

show altered RSFC in depression (Anand, Li, Wang, Wu, Gao, Bukhari, Mathews, Kalnin, & Lowe, 2005a; 2005b; Greicius et al., 2007; Zhou et al., 2010), as well as in other regions known to be involved in affective pathology (Chen et al., 2008; Johnstone et al., 2007; Matthews et al., 2008; Phillips, Drevets, Rauch, & Lane, 2003b; Urry et al., 2006). In this study we mainly found evidence for MDD-related *decreased* FC within three RSNs. These alterations have not been associated with major depression before.

First, altered FC was found in a network with regions known to be involved in emotional processing and affect regulation, such as the anterior insula, dorsal anterior cingulate cortex (dACC), ventromedial prefrontal cortex (vmPFC), temporal poles and amygdala (Pessoa, 2008). MDD patients showed strongly reduced connectivity with the amygdala within this RSN. Coupling between the vmPFC and amygdala has previously been found during downregulation of negative affect in healthy controls (Urry et al., 2006), as was reflected by decreasing amygdala activation with increasing vmPFC activation. In a similar study in depression, MDD patients showed altered coupling between these regions, potentially reflecting impaired top-down control over amygdala responses and inability to down-regulate negative affect (Johnstone et al., 2007). Involvement of the anterior insula along with dACC and somatosensory regions in this network may furthermore underscore its potential role in interoceptive awareness and emotional experience (Critchley, Wiens, Rotshtein, Ohman, & Dolan, 2004). Besides regions showing decreased FC in this RSN, the depression group also demonstrated increased connectivity of the rIFG. This region has been implicated in coping with exertion of both cognitive (Aron, Robbins, & Poldrack, 2004) and emotional (Dolcos et al., 2006) control. Recently, IFG function was found compromised in MDD when executive control had to be exerted in minimizing emotional distraction (Wang et al., 2008). Abnormal recruitment of the rIFG within the current RSN may indicate a higher propensity towards inhibition of emotional responses in depression, although the neurocircuitry to successfully do this is compromised. Taken together, the observed decoupling of the amygdala, decreased left insula connectivity, and increased rIFG connectivity within this network may be related to the impaired regulation and integration of affective responses observed in

MDD patients.

Second, we found reduced involvement of the left lateral frontal pole in a network often referred to as the TPN (Fox et al., 2005), its constituent regions commonly found activated during tasks that require cognitive effort or attention (Corbetta & Shulman, 2002). The lateral frontal poles are thought to play a key role in executive function and stimulus oriented behavior (Burgess, Dumontheil, & Gilbert, 2007a; Burgess, Gilbert, & Dumontheil, 2007b), which would complement the proposed function of this RSN. Reduced FC of the left lateral frontal pole, as was found in depression within this network, may thus reflect a suboptimally integrated attention system or reduced externally oriented attention in MDD. This abnormal connectivity pattern may relate to the cognitive deficiencies often observed in depressed patients (Ebmeier, Rose, & Steele, 2006; Rogers et al., 2004), yet this relation should be assessed in task-related imaging studies designed to address this question more directly.

Finally, we demonstrated decreased FC of the bilateral lingual gyrus in MDD in a network including ventromedial occipito-temporal areas. Although both groups showed strong connectivity with the bilateral lingual gyrus within this network, MDD patients revealed a consistent decrease in connectivity strength. Abnormalities in the visual stream are not commonly reported in MDD, and the interpretation of this effect in the depressed patients in the current study must therefore remain speculative.

In the present study we did not find abnormalities in regions previously reported to show altered RSFC in MDD. For example, increased involvement of the subgenual ACC and thalamus in the DMN has been found in MDD (Greicius et al., 2007; Zhou et al., 2010), but was not observed in the current study. Previous work furthermore reported increased connectivity of multiple brain regions within the TPN (Zhou et al., 2010). In the present study, in contrast, we showed MDD-related *reduced* connectivity of the frontal poles, which is at variance with previously found increases in connectivity in this network. In addition, support for reduced coupling between the dorsal ACC and seeds from the pallidostriatum and thalamus in MDD was not found, as has been described in previous studies (Anand, Li, Wang, Wu, Gao, Bukhari, Mathews, Kalnin, & Lowe, 2005a; 2005b).

The discrepancy in results between these studies and ours could be ascribed to differences in patient samples and analysis methods. In contrast to other studies, we report on a sample of medication-free MDD patients without comorbidity and with carefully age- and gender-matched controls. Secondly, for the current study we employed ICA analysis at the group level to obtain whole brain patterns of FC. It is conceivable that this method yields different results compared to approaches using correlations with, or between *a priori* defined regions of interest, or even when using ICA on individual data sets, although little is at present known about cross-validity between the methods.

A limitation of the present study was that our patient sample was mildly depressed on average. In addition, some patients already showed a clinically significant decrease in symptom severity because of the delay between the diagnostic assessment and the time of scanning. While this may have decreased the overall sensitivity of the study, the method applied was still successful in detecting brain functional correlates of depression, even in a mildly affected patient sample. Moreover, the effects found here were shown not to be associated with the current state of symptom severity, indicating that the observed alterations in FC may not be specific to the active state of the disorder and may not cease to exist during the remitted state.

Another limitation of the current study was the possible influence of between-group differences in heart rate variability and breathing on the results. The sampling rate used in this study (2.2 seconds per volume) was too low to avoid aliasing of these physiological signals in the data acquired. Applying temporal filtering will, therefore, not remove signal variance associated with these signals. Since physiological activity was not monitored in the current study, it remains unclear if any difference between the two groups has influenced the results. However, it has been shown that ICA is capable of detecting signal sources associated with confounding physiological signals, and that it can successfully split these from the signals of interest (Beckmann et al., 2005). We therefore think that it is unlikely that any of the differences found in this study were introduced by these physiological signals.

Because MDD-related gray matter (GM) abnormalities have been reported elsewhere (Lorenzetti et al., 2009; Sheline, 2003), we investigated whether our

MDD sample showed regions of altered GM density, potentially biasing FC within the RSNs. However, no differences were observed in average GM density between controls and patients in either of the affected RSNs as a whole, nor in the regions showing altered FC within these RSNs. In addition, GM density variance did not contribute to the altered FC patterns observed. Therefore, it is unlikely that the differences in FC were related to global or focal changes in GM density within the current study sample.

Our MDD group furthermore consisted of both first episode and recurrent episode MDD patients. Recurrence of depressive episodes can be considered an aggravation of MDD, which might cause – or conversely be caused by – an exacerbation of abnormal FC patterns. However, the small size of both subgroups, as well as the cross-sectional nature of the current study, prevented us to address this question and compare the two groups in a meaningful way. Nevertheless, follow-up data are currently being collected as part of the NESDA study. Analysis of these data should allow us to shed more light on this matter and to test whether the RSFC at baseline may have a predictive value in determining which patients are more vulnerable to develop recurrent depressive episodes. To this end, support vector classification of individual RSFC maps could be employed (Craddock et al., 2009).

In conclusion, we showed that (a history of) major depression is associated with altered FC within multiple RSNs, which could reflect less integrated processing of affective information in ventral (limbic) areas and compromised cognitive functional pathways in dorsal (PFC) regions. The current findings thereby complement previous findings on both affective and cognitive abnormalities in depression and will further increase our knowledge about the pathophysiology of the disorder.

Resting-state functional connectivity in major depression

